NISSUNA UMANA INVESTIGAZIONE SI PUO DIMANDARE VERA SCIENZIA
S'ESSA NON PASSA PER LE MATEMATICHE DIMOSTRAZIONI
LEONARDO DA VINCI

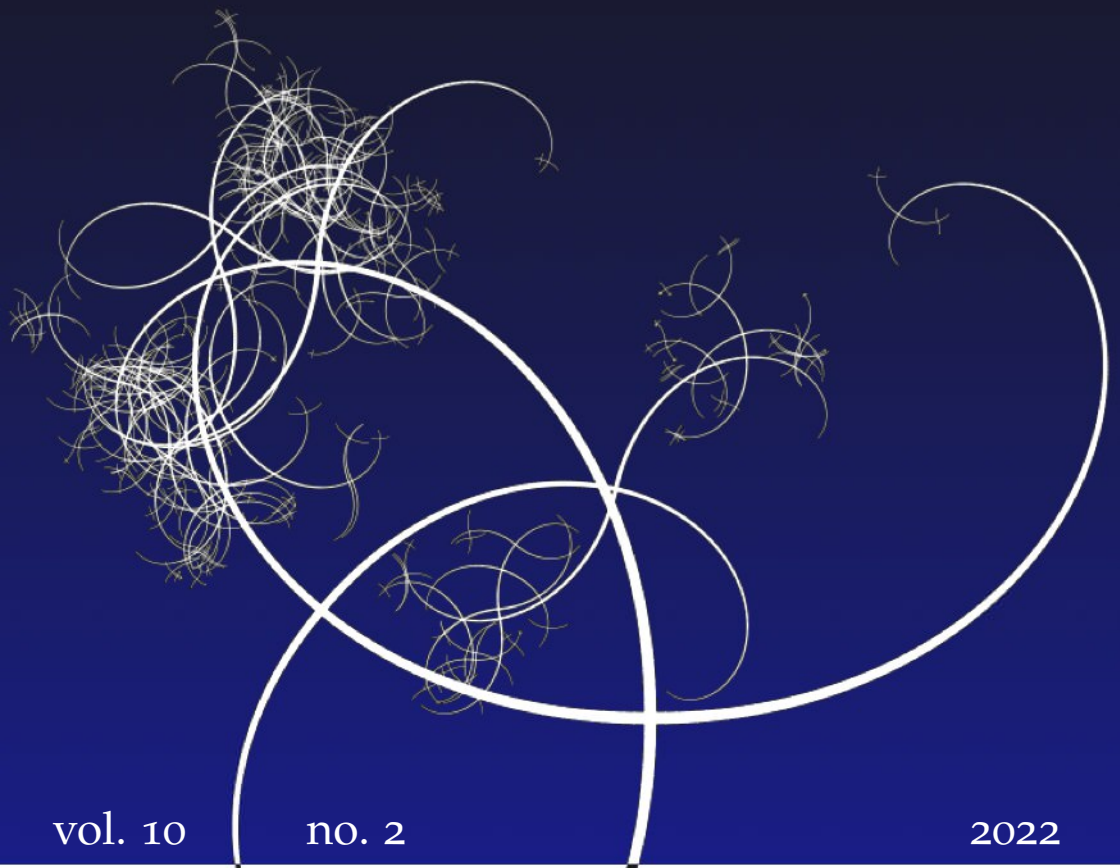

vol. 10 no. 2 2022

Mathematics and Mechanics *of* Complex Systems

Mallinath Dhange, Gurunath Sankad and Umesh Bhujakkanavar

MODELING OF BLOOD FLOW WITH STENOSIS AND DILATATION

msp

MATHEMATICS AND MECHANICS OF COMPLEX SYSTEMS
Vol. 10, No. 2, 2022
https://doi.org/10.2140/memocs.2022.10.155

MODELING OF BLOOD FLOW WITH STENOSIS AND DILATATION

MALLINATH DHANGE, GURUNATH SANKAD AND UMESH BHUJAKKANAVAR

The stenosis of an artery lowers blood flow in the artery. This stenosed artery induces tangential pressure stress, which weakens the arterial wall and leads to dilatation or aneurysm. This article examines blood flow through an inclined tube with stenosis and expansion after stenosis (dilation) under the effect of a steady incompressible Casson fluid flow. The mechanically regulated stenosis formation and post-stenotic dilatation in blood vessels were studied by using a mild stenosis approximation and appropriate boundary conditions. Expressions for velocity, pressure drop, wall shear stress, and flow resistance are derived analytically. The impact of various physical parameters on fluid resistance to flow and wall shear stress is investigated. The wall shear stress and the impedance of the flow increase for the height of stenosis and decrease for the height of dilatation with a rise in the angle of proclivity. It is seen that the plug flow radius is more in the case of the inclined artery as compared to the noninclined artery.

A list of symbols can be found on page 167.

1. Introduction

The term stenosis refers to a constriction of an artery caused by arteriosclerotic deposition or other abnormal tissue growth. Blood flow is obstructed as the development progresses into the artery's lumen. The obstruction may cause damage to the inner cells of the wall, leading to stenosis progression. The development of stenosis and the flow of blood through the artery are thus linked, since each affects the other. The progression of stenosis in an artery can have serious consequences and disrupt the normal functioning of the circulatory system. Specifically, it might prompt increased resistance to flow with the possible serious decrease in blood flow; increased risk of complete occlusion; abnormal cell development in the region of the stenosis, which builds the intensity of the stenosis; and tissue harm prompting post-stenosis dilatation.

The study of blood flow through stenosed veins is a key topic of research since circularity issues cause more than 30% of all deaths, and these circularity issues can

Communicated by Anil Misra.
MSC2020: 76D05, 76D99, 76Z05, 92C10.
Keywords: stenotic artery, dilatation, Casson fluid, impedance, wall shear stress.

induce symptoms such as chest pain and a reduction in blood supply to the brain. The failure of the cardiovascular system increases the risk of death. Stenosis is the most common cause of circularity problems. A typical cardiovascular ailment is a stenotic artery, which restricts blood flow. The normal function of the cardiac system might be affected by stenosis. It also raises blood pressure and causes tissue damage, which leads to stenotic dilatation. Young [35] was the first to investigate stenosis and studied the time-dependent stenosis effects on the flow of blood through a tube. Azuma and Fukushima [1] modeled the flow patterns in stenosed blood vessels. The effects of vascular stenosis on steady flow were observed by MacDonald [11]. Following that, several researchers studied the flow characteristics of blood in a tube with mild constriction by using blood as Newtonian or non-Newtonian fluids in a variety of conditions [2; 5; 6; 7; 14; 16; 25; 26; 28].

Scientists have been particularly interested in studying the non-Newtonian nature of blood flow because of its use in studying the flow of blood via narrow arteries. The Newtonian fluid, micropolar, Herschel–Bulkley, and Jeffrey models are used in the majority of studies in the literature. Because of the presence of yield stress, this technique fails to clarify the physiological conduct of the bloodstream in supply routes. Even though the Herschel–Bulkley fluid has a yield stress limitation, the Casson model matches the blood flow better at low shear rates than the Herschel–Bulkley fluid (see Scott Blair [3]). In recent years, many researchers have investigated Casson fluid in various physiological circumstances [8; 23; 32].

Many ducts in physiological systems are known to be inclined to the axis rather than horizontal. The blood flow through an artery with numerous stenosis and a nonuniform cross-section was studied by Prasad and Radhakrishnamacharya [13]. Umadevi et al. [31] investigated the blood flow in an inclined overlapping stenosed artery with a magnetic field combined with copper nanoparticles.

Post-stenotic dilatation refers to arterial dilatation that occurs after a stenosis has developed. It has been observed that certain people's nerve systems are weak (especially in old people). When blood clots in a specific location, the artery wall bulges out from that location due to high pressure. If it continues to rise, the artery walls may be damaged. It may result in death. Although the specific cause of post-stenotic dilatation is unknown, increased lateral pressure, cavitation, anomalous shear stresses, and turbulence have all been proposed. As a result, a better understanding of dilatation issues will aid in the diagnosis of arterial disorders. Pincombe et al. [17] investigated the effects of post-stenotic dilatations on blood flow through stenosed coronary arteries because of their importance. Priyadharshini and Ponalagusamy [21] examined the flow of Herschel–Bulkley fluid through tapered artery stenosis and dilatation using a biorheological model. The effects of post-stenotic dilatation on the flow of couple stress fluid via stenosed arteries were investigated by Prasad et al. [19]. Sharma et al. [24] and Verma and Parihar [33]

investigated the effect of a constant external magnetic field in a multistage stenosis artery in the central region, hypothesizing that the yield stress and stenosis reduce the shear stress of the wall and the flow speed within the magnetic field's sight. Several experts have recently looked into the characteristics of blood flow through the artery in the presence of stenosis [4; 9; 10; 12; 18; 22; 27; 30; 34].

With this in mind, an attempt was made to investigate the effects of stenosis and post-stenotic dilatation on a Casson fluid with mild stenosis conditions. The research is carried out analytically. It is possible that a growth in the extent of the stenosis in the artery disturbed the normal flow of blood through vessels in the heart, body, and brain, and that this might lead to significant cardiac disease problems such as stroke, heart attack, and so on. The mathematical model described here may help and support the physician in understanding the biomechanical effects that lead to artery stenosis and damage. It proposes a new approach to preventing atherosclerosis.

2. Formulation of the problem and its solution

Consider the flow of an incompressible Casson fluid through an inclined axisymmetric stenosed artery (tube) of the uniform cross-section with post-stenotic dilatations. The stenosis is supposed to be mild and develop in an axially symmetric manner. The geometry of the wall is as shown in Figure 1.

The equation relating the geometry of the wall is (Pincombe et al. [17])

$$h(z) = \frac{R}{R_0} = \begin{cases} 1 - \dfrac{\delta_i}{2R_0}\left(1 + \cos\dfrac{2\pi}{L_i}\left(z - \alpha_i - \dfrac{L_i}{2}\right)\right), & \alpha_1 \le z \le \beta_i, \\ 1, & \text{otherwise.} \end{cases} \tag{1}$$

Here, δ_i is how far the i-th abnormal segment projects into the lumen. It is positive

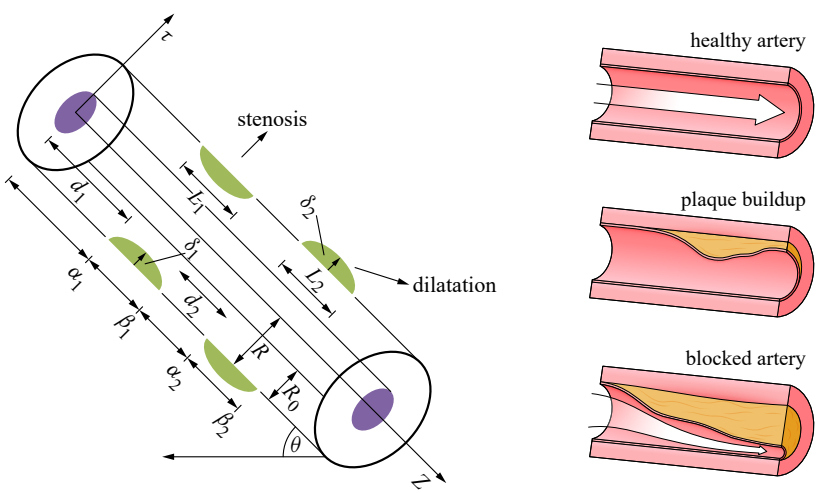

Figure 1. Schematic diagram of the tube with stenosis.

for stenosis and negative for aneurysms. L_i is the length of the i-th abnormal segment, R is the radius of the artery, R_0 is the radius of the normal artery, α_i is the distance between the origin and the beginning of the i-th abnormal segment.

The distance from the origin to the beginning of the i-th abnormal segment is

$$\alpha_i = \Big(\sum_{j=1}^{i} (d_j + L_j) \Big) - L_i, \tag{2}$$

where d_i is the distance from the start of the i-th diseased segment from the end of the $(i-1)$-st segment.

The distance from the origin to the end of the i-th abnormal segment (β_i) is

$$\beta_i = \sum_{j=1}^{i} (d_j + L_j). \tag{3}$$

From [19] and [25], we adopt the following limitations for mild stenosis:

$$\min(R_0, R_{\text{out}}) \gg \delta_1, \delta_2 \quad \text{and} \quad L_1, L_2 \gg \delta_1, \delta_2, \quad \text{where } R(z) = R_{\text{out}} \text{ at } z = L.$$

Governing equations. In this study, blood is supposed to be a homogeneous and incompressible non-Newtonian fluid. The viscosity of blood can be described using a variety of non-Newtonian models, such as the power-law model, the micropolar fluid model, and the Herschel–Bulkley fluid model. In this investigation, we used the Casson model to describe the material property of blood viscosity because, when compared to other viscosity models, the Casson model accurately represents the viscosity properties of physiological blood in real life (Pratumwal et al. [20]).

The expression of the Casson model, taken from Prasad and Radhakrishnamacharya [13] and Pincombe et al. [17], is

$$\frac{1}{r}\frac{\partial}{\partial r}(r\tau_{rz}) = -\frac{1}{\mu}\frac{\partial p}{\partial z} + \rho g \sin\theta, \tag{4}$$

where

$$\sqrt{\tau_{rz}} = \begin{cases} \sqrt{\mu}\sqrt{-\partial u/\partial r} + \sqrt{\tau_0}, & \tau \geq \tau_0, \\ 0, & \tau \leq \tau_0. \end{cases} \tag{5}$$

Here, τ_{rz} is the shear stress, μ is the blood viscosity, ρ is the density, g is the acceleration of gravity, θ is the angle of inclination, p is the pressure, τ_0 is the yield stress, and r, z are the radial and axial coordinates.

Considering the forces in the plug region, we get

$$2\pi r_0 B\tau_0 = P\pi r_0^2 B \qquad \therefore \tau_0 = \frac{Pr_0}{2}, \quad \text{where } P = \frac{\partial p}{\partial z}. \tag{6}$$

Boundary conditions and numerical solution. Boundary conditions are important in computing the solutions to simulated physical problems. Considering that the blood particles adhere to the inner surface of the arterial segment under consideration, the axial velocity (u) of blood particles on the wall surface, corresponding to one-dimensional flow, may be taken to be equal to the velocity of the vascular wall

material points along the same direction. For the stenosed portion, this may be stated mathematically as

$$u = 0 \text{ at } r = h. \tag{7}$$

The velocity gradient of the fluid flow along the axis can be considered to be zero, implying that there is no fluid shear rate along the axis of the artery segment under consideration, which can be represented as

$$\tau_{rz} \text{ is finite at } r = 0. \tag{8}$$

About half of the patients who had mild to moderate stenosis at the start of the study experienced increasing valve calcification, resulting in hemodynamically severe aortic stenosis symptoms. In mild stenosis conditions, the flaps (cusps) of the aortic valve may become thickened and stiff, or they may fuse. This causes narrowing of the aortic valve opening. The narrowed valve isn't able to open fully, which reduces or blocks blood flow from the heart into the aorta and the rest of the body (see Ott [15]).

Using the mild stenosis restriction and solving equation (4) under the boundary conditions (7) and (8), the fluid velocity is given as

$$u = \frac{P+f}{2\mu}\left(\tfrac{4}{3}r_0^{1/2}\left(r^{3/2}-h^{3/2}\right) - \tfrac{1}{2}(r^2-h^2) - r_0(r-h)\right). \tag{9}$$

Substituting $r = r_0$ in this equation, we get the plug velocity as

$$u_p = \frac{P+f}{2\mu}\left(-\tfrac{1}{6}r_0^2 - \frac{4}{3}r_0^{1/2}h^{3/2} + \tfrac{1}{2}h^2 + hr_0\right), \tag{10}$$

where $f = \sin\alpha/F$ and $F = (\mu u^{1/2})/(\rho g R_0^{3/2})$.

The fluid's flow flux Q is defined as

$$Q = 2\int_0^{r_0} u_p r\,dr + 2\int_{r_0}^{h} ur\,dr. \tag{11}$$

Therefore,

$$Q = \frac{P+f}{\mu}\left(-\tfrac{1}{168}r_0^4 - \tfrac{2}{7}r_0^{1/2}h^{7/2} + \tfrac{1}{8}h^4 + \tfrac{1}{6}h^3 r_0\right). \tag{12}$$

The nondimensional quantities are

$$\begin{aligned}
&r' = \frac{r}{R_0}, \quad r_0' = \frac{r_0}{R_0}, \quad \delta_1' = \frac{\delta_1}{R_0}, \quad \delta_2' = \frac{\delta_2}{R_0}, \quad H = \frac{h}{R_0},\\
&z' = \frac{z}{L}, \quad L_1' = \frac{L_1}{L}, \quad L_2' = \frac{L_2}{L}, \quad u = \frac{u'}{U_0}, \quad d_1' = \frac{d_1}{L},\\
&d_2' = \frac{d_2}{L}, \quad Q' = \frac{Q}{U_0 R_0^2}, \quad p' = \frac{p}{(\mu U_0 B)/R_0^2}, \quad r_0' = \frac{r_0}{R_0}, \quad r' = \frac{r}{R_0}.
\end{aligned} \tag{13}$$

From (12) and (13), we get

$$Q = (P+f)\left[-\tfrac{1}{168}r_0^4 - \tfrac{2}{7}r_0^{1/2}H^{7/2} + \tfrac{1}{8}H^4 + \tfrac{1}{6}H^3 r_0\right]. \tag{14}$$

Equation (14) can be expressed as

$$\frac{\partial p}{\partial z} = -\frac{Q}{\left[-\tfrac{1}{168}r_0^4 - \tfrac{2}{7}r_0^{1/2}H^{7/2} + \tfrac{1}{8}H^4 + \tfrac{1}{6}H^3 r_0\right]} + f. \tag{15}$$

The primitive of (15) gives the pressure difference $\triangle p$ along the total length of the channel as

$$\triangle p = \int_0^1 \frac{\partial p}{\partial z}\,dz = \int_0^1 \left\{\frac{-Q}{\left[-\tfrac{1}{168}r_0^4 - \tfrac{2}{7}r_0^{1/2}H^{7/2} + \tfrac{1}{8}H^4 + \tfrac{1}{6}H^3 r_0\right]} + f\right\} dz. \tag{16}$$

A definition of flow resistance is

$$\lambda = \frac{\triangle p}{Q}. \tag{17}$$

From equations (16) and (17), we get

$$\lambda = \frac{1}{Q}\int_0^1 \left\{\frac{-Q}{\left[-\tfrac{1}{168}r_0^4 - \tfrac{2}{7}r_0^{1/2}H^{7/2} + \tfrac{1}{8}H^4 + \tfrac{1}{6}H^3 r_0\right]} + f\right\} dz. \tag{18}$$

The pressure drop is calculated as follows in the absence of stenosis ($H = 1$):

$$(\triangle p)_n = \int_0^1 \left\{\frac{-Q}{\left[-\tfrac{1}{168}r_0^4 - \tfrac{2}{7}r_0^{1/2} + \tfrac{1}{8} + \tfrac{1}{6}r_0\right]} + f\right\} dz. \tag{19}$$

Flow resistance is defined as follows in the absence of stenosis:

$$\lambda_n = \frac{(\triangle p)_n}{Q}. \tag{20}$$

From (19) and (20), we obtain

$$\lambda_n = \frac{1}{Q}\int_0^1 \left\{\frac{-Q}{\left[-\tfrac{1}{168}r_0^4 - \tfrac{2}{7}r_0^{1/2} + \tfrac{1}{8} + \tfrac{1}{6}r_0\right]} + f\right\} dz. \tag{21}$$

The normalized resistance of a flow is defined as

$$\bar{\lambda} = \frac{\lambda}{\lambda_n}. \tag{22}$$

The shear stress acting on the channel's wall is determined by

$$\tau_w = -\mu \frac{\partial u}{\partial r}\bigg|_{r=h}. \tag{23}$$

Applying the dimensional quantities from (13) to (23) we get

$$\tau_w' = \frac{\tau_w}{[(\mu U)/R_0]}. \tag{24}$$

Equation (24) reduces to

$$\tau_w' = -\frac{\partial u'}{\partial r'}. \tag{25}$$

Using equations (9) (in nondimensional form) and (15) in (25), we get

$$\tau_w = \frac{-Q}{2}\left\{\frac{2r_0^{1/2}H^{1/2} - H - r_0}{\frac{1}{168}r_0^4 + \frac{2}{7}r_0^{1/2}H^{7/2} - \frac{1}{8}H^4 - \frac{1}{6}H^3 r_0}\right\} + f. \tag{26}$$

In the absence of stenosis ($H = 1$), the shear stress at the wall is calculated using (26) as follows:

$$(\tau_w)_n = \frac{-Q}{2}\left\{\frac{2r_0^{1/2} - 1 - r_0}{\frac{1}{168}r_0^4 + \frac{2}{7}r_0^{1/2} - \frac{1}{8} - \frac{1}{6}H^3 r_0}\right\} + f. \tag{27}$$

The normalized shear stress at the wall can be calculated as

$$\bar{\tau}_w = \frac{\tau_w}{(\tau_w)_n}. \tag{28}$$

3. Numerical results and discussion

The study of the physiology and anatomy of a biological system depends on the knowledge of the blood flow through arteries. The progress and cause of various arterial diseases are related to the mechanical behavior and the flow characteristics of blood vessel walls. The unnatural and abnormal growth in the arterial wall thickness at different locations of the cardiovascular system is medically termed stenosis. Its presence in one or more places restricts blood flow across the coronary arteries' lumen. Once the decrease has reached maturity, it causes major changes in blood flow, such as flow resistance and wall shear stress. Resistance to flow and wall shear stress are important variables in the study of blood flow through a stenosed artery and post-stenotic dilatation. Analytical solutions for the velocity of the fluid (u), flow resistance ($\bar{\lambda}$) and wall shear stress ($\bar{\tau}_w$) were given in equations (9), (22), and (28). The effects of several parameters on flow resistance, wall shear stress and fluid velocity were computed and plotted using Mathematica.

Resistance to the flow. Figures 2–4 show the impedance behavior on a variety of parameters including stenosis height (δ_1) and height of the dilatation (δ_2). It is noticed that increase in the radial distance (r) of the plug region, the impedance of the flow ($\bar{\lambda}$) rises in the case of stenosis height (Figure 2, top) but drops in the case of dilatation height (Figure 2, bottom). Figure 3 illustrates that the impedance ascends concerning the height of the stenosis and descends for the height of dilation as the angle of proclivity increases. There is a significant change in the plug flow radius in the inclined artery, which influences the flow due to the smaller lumen size. When comparing inclined arteries to noninclined arteries, the plug flow radius

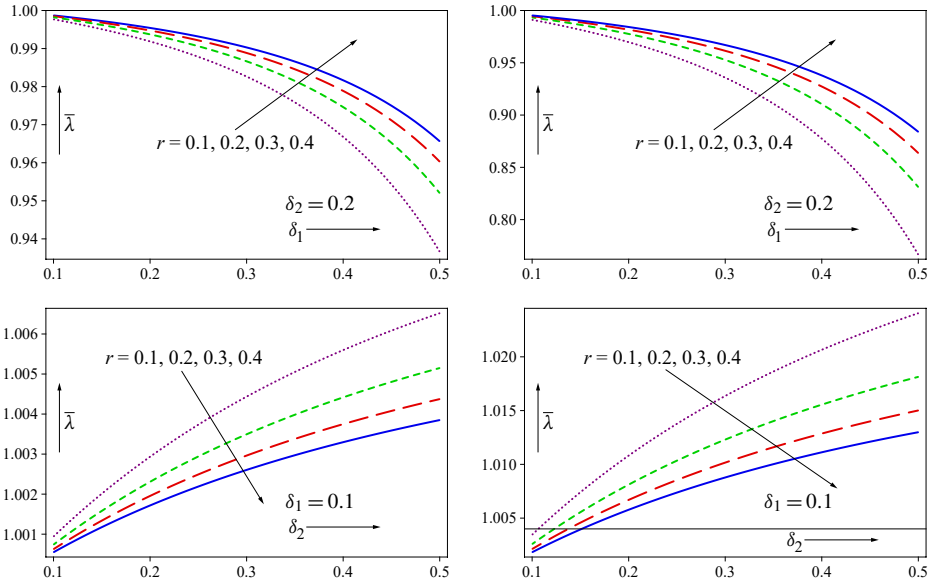

Figure 2. Variation of $\bar{\lambda}$ with δ_1 and r (top) or δ_2 and r (bottom), for $d_1 = 0.2$, $d_2 = 0.6$, $L_1 = L_2 = 0.2$, $Q = 0.1$, $\theta = \pi/6$, $F = 0.1$ (left) and $F = 0.3$ (right).

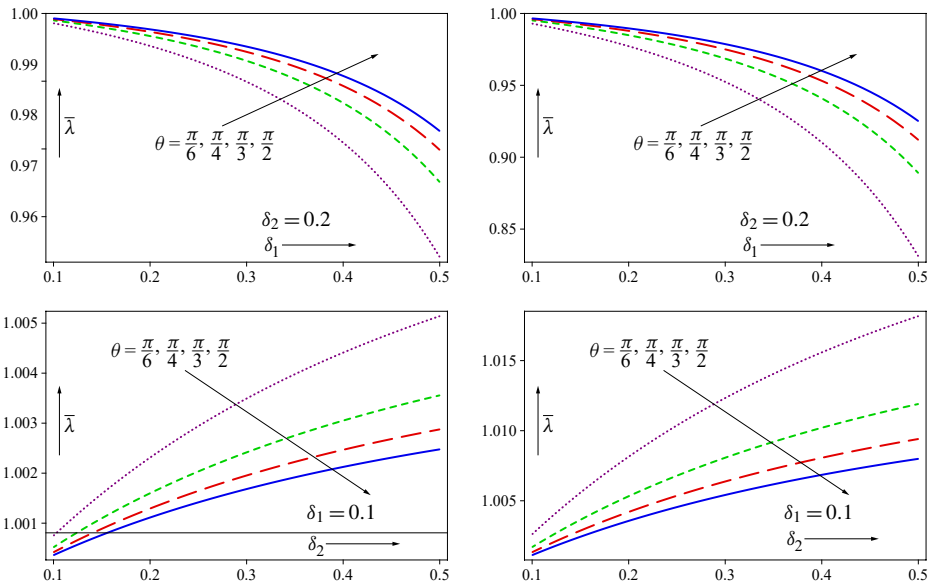

Figure 3. Variation of $\bar{\lambda}$ with δ_1 and θ (top) or δ_2 and θ (bottom), for $d_1 = 0.2$, $d_2 = 0.6$, $L_1 = L_2 = 0.2$, $Q = 0.1$, $\theta = \pi/6$, $F = 0.1$ (left) and $F = 0.3$ (right).

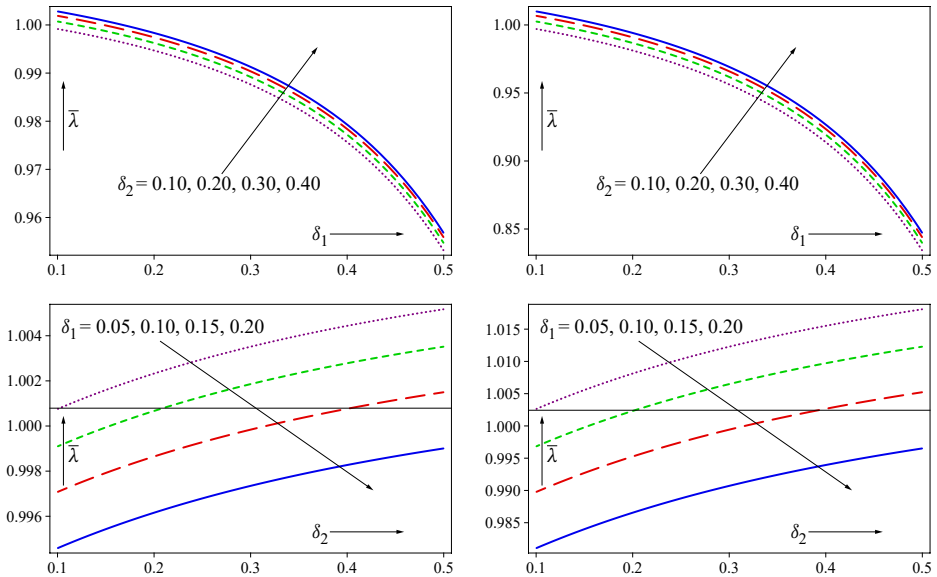

Figure 4. Variation of $\bar{\lambda}$ with δ_1 and δ_2 (two views, top and bottom), for $d_1 = 0.2$, $d_2 = 0.6$, $L_1 = L_2 = 0.2$, $Q = 0.1$, $\theta = \pi/6$, $r = 0.2$, $F = 0.1$ (left) and $F = 0.3$ (right).

is larger in inclined arteries. This is in agreement with Srivastava [29].

In Figure 4 it is seen that resistance to flow increases with the dilation height, but decreases with a rise in height of the stenosis. Resistance to flow is found to yield higher values for the arteries with higher stenosis heights, but the opposite is true for the arteries with lower stenosis heights. It's important to note the physical cause of these observations. The blocked fluid in the stenosis region quickly moves towards the main flow region. As a result, the fluid has a temporary resistance to flow in the pre-stenotic region before reaching its minimum in the post-stenotic region. The results from our are in agreement with those of [13] and [21].

Wall shear stress. Figures 5–7 illustrate the effect on wall shear stress ($\bar{\tau}_w$) of the stenosis height (δ_1) and dilatation height (δ_2). From Figure 5 we observe that wall shear stress decreases and increases concerning the height of stenosis and dilatation, respectively, as the radial distance (r) of the plug flow region increases. In Figure 6 we see that with an increase in proclivity angle (θ), the shear stress grows in the case of stenosis height but decreases in the case of the dilatation height. Figure 7 illustrates that shear stress increases with an increase in dilatation height but decreases with an increase in stenosis height. The results obtained with our model in the case of wall shear stress are similar to those obtained by Young [35], Prasad and Radhakrishnamacharya [13], and Pincombe et al. [17].

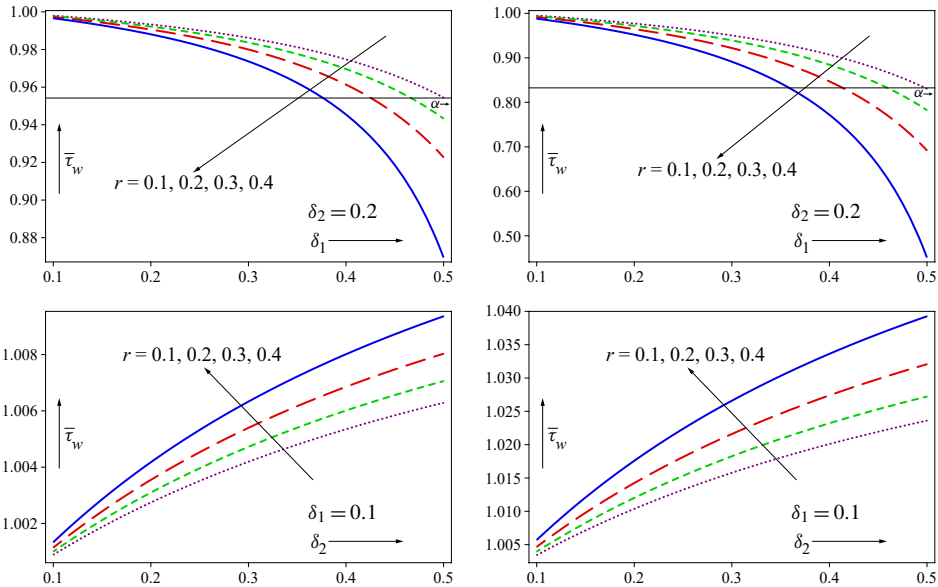

Figure 5. Variation of $\bar{\tau}_w$ with δ_1 and r (top) or δ_2 and r (bottom), for $d_1 = 0.2$, $d_2 = 0.6$, $L_1 = L_2 = 0.2$, $Q = 0.1$, $\theta = \pi/6$, $F = 0.1$ (left) and $F = 0.3$ (right).

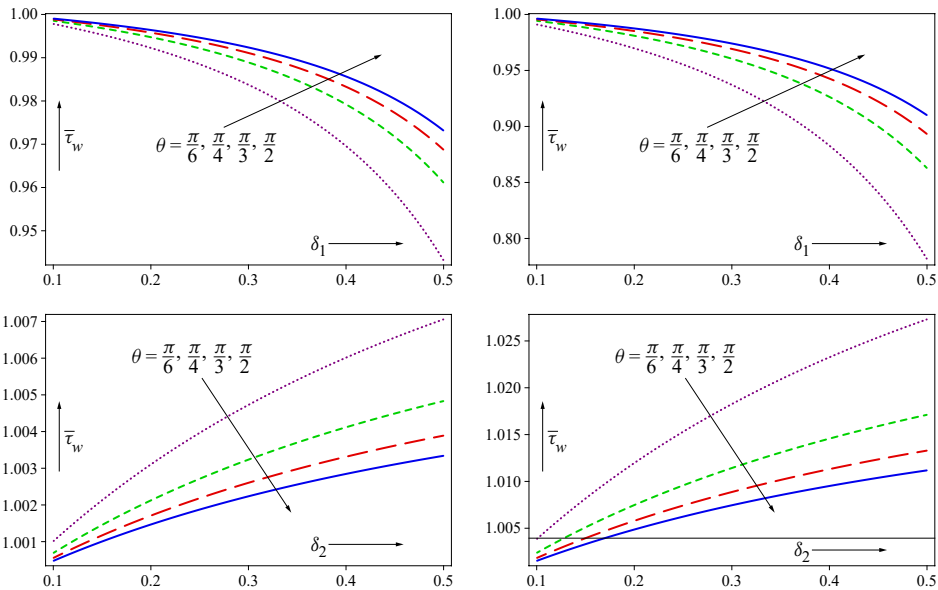

Figure 6. Variation of $\bar{\tau}_w$ with δ_1 and θ (top) or δ_2 and θ (bottom), for $d_1 = 0.2$, $d_2 = 0.6$, $L_1 = L_2 = 0.2$, $Q = 0.1$, $r = 0.2$, $F = 0.1$ (left) and $F = 0.3$ (right).

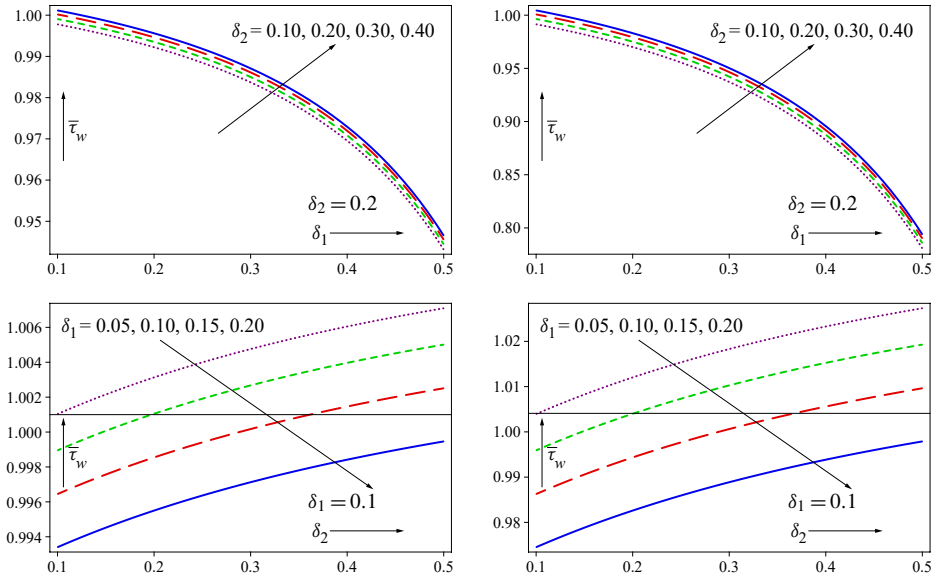

Figure 7. Variation of $\bar{\tau}_w$ with δ_1 and δ_2 (two views, top and bottom), for $d_1 = 0.2$, $d_2 = 0.6$, $L_1 = L_2 = 0.2$, $Q = 0.1$, $\theta = \pi/6$, $r = 0.2$, $F = 0.1$ (left) and $F = 0.3$ (right).

Understanding wall shear stress is an important part of the study of small arteries and arterioles. The pressure gradient and wall shear stress have a substantial impact on the arteries, which grow quite hard and lose their flexibility over time. When these affected arteries are subjected to excessive blood pressure, the arterial wall ruptures.

Velocity of fluid. The effects of several parameters on the velocity of the fluid (u) are shown in Figures 8 and 9. It is seen that fluid velocity increases with the dilatation height (δ_2) (Figure 8, top) and decreases with the stenosis height (δ_1) (Figure 8, bottom). The velocity rises with the angle of proclivity (θ) for both the cases of stenosis (Figure 9). Specifically, increasing the proclivity leads to a decrease in velocity at the boundary of the arterial wall, but the velocity in the center of the arterial tube increases with the height of the stenosis and dilation, implying an increase in the viscous forces near the artery wall. These results are consistent with those of Young [35] and Prasad and Radhakrishnamacharya [13].

4. Concluding remarks

The mathematical model of Casson fluid in a steady-state and incompressible in a uniform tube with stenosis and expansion after stenosis is analyzed. The governing equations describing the transport phenomena relevant to our model are solved by

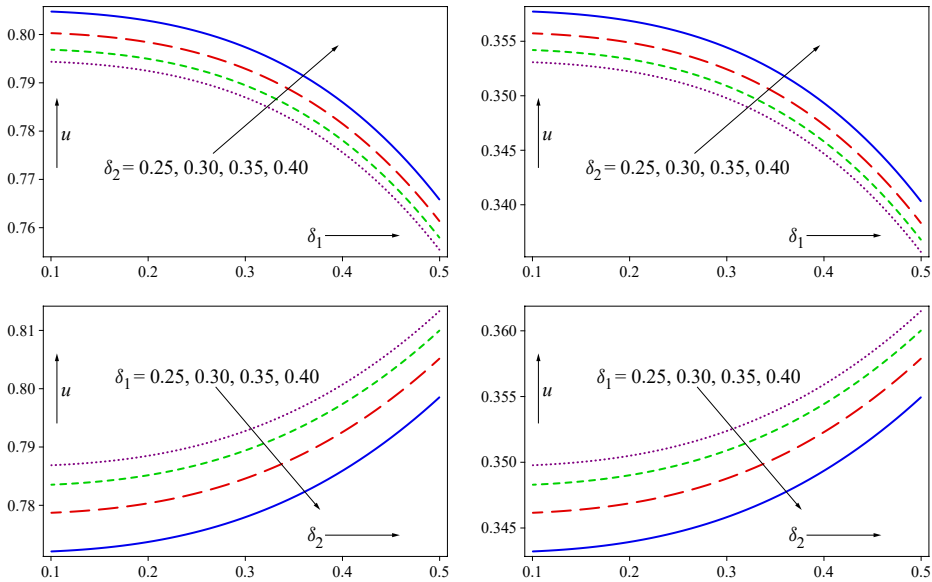

Figure 8. Variation of u with δ_1 and δ_2 (two views, top and bottom), for $d_1 = 0.2$, $d_2 = 0.6$, $L_1 = L_2 = 0.2$, $Q = 0.1$, $\theta = \pi/6$, $r = 0.2$, $F = 0.1$ (left) and $F = 0.3$ (right).

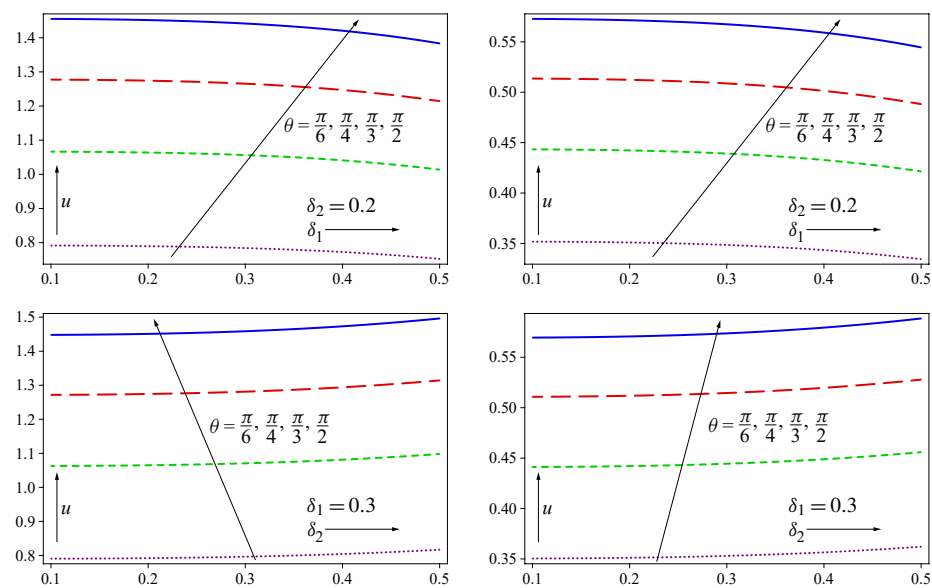

Figure 9. Variation of u with δ_1 and θ (top) or δ_2 and θ (bottom), for $d_1 = 0.2$, $d_2 = 0.6$, $L_1 = L_2 = 0.2$, $Q = 0.1$, $F = 0.1$ (left) and $F = 0.3$ (right).

using mild stenosis and boundary conditions. For different values of radial distance, angle of inclination, the height of stenosis, and expansion after stenosis, the results obtained are presented graphically. The main findings are listed below:

- In the case of stenosis, flow impedance ($\bar{\lambda}$) increases and wall shear stress ($\bar{\tau}_w$) decreases as the radial distance of the plug flow region (r) increases. By contrast, in the case of post-stenotic dilatation, $\bar{\lambda}$ decreases and $\bar{\tau}_w$ increases with an increase in r.
- With a rise in the angle of proclivity (θ), flow impedance and shear stress increase with respect to stenosis height (δ_1) and decrease with respect to dilatation height (δ_2).
- With an increase in stenosis height, flow impedance and wall shear stress both decrease. By contrast, with an increase in dilatation height, flow impedance and wall shear stress increase.
- Fluid velocity (u) decreases as stenosis height increases, but it rises with an increase in dilatation height.
- Fluid velocity increases with proclivity angle for stenosis and dilatation.
- The mathematical model described here may help and support physicians in getting the mathematical knowledge needed for medicinal applications.

List of symbols

L	length of the channel (m)	$\bar{\lambda}$	resistance to flow ($\mathrm{kg/m^4s}$)
L_1	length of stenosis (m)	$\bar{\tau}_w$	wall shear stress ($\mathrm{N/m^2}$)
L_2	length of post-stenotic dilatation (m)	τ_{rz}	shear stress ($\mathrm{N/m^2}$)
δ_1	max height of stenosis (m)	μ	blood viscosity ($\mathrm{kg/ms}$)
δ_2	max height of post-stenotic dilatation (m)	τ_0	yield stress ($\mathrm{N/m^2}$)
r	radial coordinate (m)	z	axial coordinate (m)
θ	angle of proclivity (radian)	p	pressure in the region ($\mathrm{kg/ms^2}$)
$R(z)$	radius of the artery (m)	$R_0(z)$	radius of normal artery (m)

Acknowledgments

The authors are grateful for helpful comments from all reviewers, which have led to a marked improvement in the manuscript.

References

[1] T. Azuma and T. Fukushima, "Flow patterns in stenotic blood vessel models", *Biorheology* **13**:6 (1976), 337–3555.

[2] R. Bali and U. Awasthi, "A Casson fluid model for multiple stenosed artery in the presence of magnetic field", *Appl. Math.* (*Irvine*) **3**:5 (2012), 436–441.

[3] G. Blair, "An equation for the flow of blood, plasm and serum through glass capillaries", *Nature* **183** (1959), 613–614.

[4] S. Chakravarty and A. Datta, "Effects of stenosis on arterial rheology through a mathematical model", *Math. Comput. Model.* **12**:12 (1989), 1601–1612.

[5] P. Chaturani and R. PonnalaguSamy, "Pulsatile flow of Casson's fluid through stenosed arteries with applications to blood flow", *Biorheology* **23**:5 (1986), 499–511.

[6] J. H. Forrester and D. F. Young, "Flow through a conversing diverging tube and its implications in occlusive vascular disease, I: Theoretical development", *J. Biomech.* **3**:3 (1970), 297–305.

[7] J. H. Forrester and D. F. Young, "Flow through a conversing diverging tube and its implications in occlusive vascular disease, II: Theoretical and experimental results and their implications", *J. Biomech.* **3**:3 (1970), 307–316.

[8] M. Gudekote and R. Choudhari, "Slip effect on peristaltic transport of Casson fluid in an inclined elastic tube with porous walls", *J. Adv. Res. Fluid Mech. Therm. Sci.* **43**:1 (2018), 67–80.

[9] A. K. Gupta and G. D. Gupta, "Unsteady blood flow in an artery through a non-symmetrical stenosis", *Acta Cienc. Indica Math.* **27**:2 (2001), 137–142.

[10] H. Kumar, R. S. Chandel, S. Kumar, and S. Kumar, "A mathematical model for different shapes of stenosis and slip velocity at the wall through mild stenosis artery", *Adv. Appl. Math. Biosci.* **5**:1 (2014), 9–18.

[11] D. A. MacDonald, "On steady flow through modelled vascular stenosis", *J. Biomech.* **12**:1 (1979), 13–20.

[12] P. K. Mandal, "An unsteady analysis of non-Newtonian blood flow through tapered arteries with a stenosis", *Int. J. Non-Linear Mech.* **40**:1 (2005), 151–164.

[13] K. Maruthi Prasad and G. Radhakrishnamacharya, "Flow of Herschel–Bulkley fluid through an inclined tube of non-uniform cross-section with multiple stenoses", *Arch. Mech.* **60**:2 (2008), 161–172.

[14] J. C. Misra and B. K. Kar, "Momentum integral method for studying flow characteristics of blood through a stenosed vessel", *Biorheology* **26**:1 (1989), 23–35.

[15] C. Otto, "Aortic stenosis: Even mild disease is significant", *Eur. Heart J.* **25**:3 (2004), 185–187.

[16] J. Perkkiö and R. Keskinen, "On the effect of the concentration profile of red cells on blood flow in the artery with stenosis", *Bull. Math. Biol.* **45**:2 (1983), 259–267.

[17] B. Pincombe, B. Mazumdar, and J. Hamilton-Craig, "Effects of multiple stenoses and post-stenotic dilation on non-Newtonian blood flow in small arteries", *Med. Biol. Eng. Comput.* **37**:5 (1999), 595–599.

[18] R. N. Pralhad and D. H. Schultz, "Modeling of arterial stenosis and its applications to blood diseases", *Math. Biosci.* **190**:2 (2004), 203–220.

[19] K. M. Prasad, T. Sudha, and M. V. Phanikumar, "The effects of post-stenotic dilatation on the flow of couple stress fluid through stenosed arteries", *Am. J. Comput. Math.* **6**:4 (2016), 365–376.

[20] Y. Pratumwal, W. Limtrakaran, S. Muengtaweepongsa, P. Phakdeesan, and K. Intharakham, "Whole blood viscosity modelling using power law, Casson, and Carreau Yasuda models intergrated with image scanning u-tube viscometer technique", *Songklanakarin J. Sci. Tech.* **39**:5 (2017), 625–631.

[21] S. Priyadharshini and R. Ponalagusamy, "Biorheological model on flow of Herschel–Bulkley fluid through a tapered arterial stenosis and dilatation", *Appl. Bionics Biomech.* **2015** (2015), art. id. 406195.

[22] J. V. Ramana-Reddy and D. Srikanth, "Impact of blood vessel wall flexibility on the temperature and concentration dispersion", *J. Appl. Comput. Mech.* **6**:3 (2020), 564–581.

[23] G. Sankad and M. Dhange, "Effect of chemical reactions on dispersion of a solute in peristaltic motion of Newtonian fluid with wall properties", *Malays. J. Math. Sci.* **11**:3 (2017), 347–363.

[24] M. K. Sharma, P. R. Sharma, and V. Nasha, "Pulsatile MHD arterial blood flow in the presence of double stenosis", *J. Appl. Fluid Mech.* **6**:3 (2013), 331–338.

[25] J. B. Shukla, R. S. Parihar, and B. Rao, "Effects of stenosis on non-Newtonian flow through an artery with mild stenosis", *Bull. Math. Biol.* **42** (1980), 283–294.

[26] D. S. Srinivasacharya and D. Srikanth, "Effect of couple stresses on the flow in a constricted annulus", *Arch. Appl. Mech.* **78** (2008), 251–257.

[27] L. M. Srivastava, "Flow of couple stress fluid through stenotic blood vessels", *J. Biomech.* **18**:7 (1985), 479–485.

[28] V. P. Srivastava, "Flow of a couple stress fluid representing blood through stenotic vessels with a peripheral layer", *Indian J. Pure Appl. Math.* **34** (2003), 1727–1740.

[29] N. Srivastava, "The Casson fluid model for blood flow through an inclined tapered artery of an accelerated body in the presence of magnetic field", *Int. J. Bio. Eng. Tech.* **15** (2014), 198–210.

[30] P. N. Tandon, U. V. Rana, M. Kawahara, and V. K. Katiyar, "A model for blood flow through stenotic tube", *Int. J. Biomed. Comput.* **32**:1 (1993), 62–78.

[31] C. Umadevi, M. Dhange, B. Haritha, and T. Sudha, "Flow of blood mixed with copper nanoparticles in an inclined overlapping stenosed artery with magnetic field", *Case Stud. Therm. Eng.* **25** (2021), art. id. 100947.

[32] K. Vajravelu, S. Sreenadh, P. Devaki, and K. V. Prasad, "Peristaltic pumping of a Casson fluid in an elastic tube", *J. Appl. Fluid Mech.* **9**:4 (2016), 1897–1905.

[33] N. Verma and R. S. Parihar, "Effect of magneto-hydrodynamics and haematocrit on blood flow in an artery with multiple mild stenosis", *Int. J. Appl. Math. Comput.* **1** (2009), 30–46.

[34] G. Yasodhara, S. Sreenadh, B. Sumalatha, and A. Srinivas, "Axisymmetric peristaltic flow of a non-Newtonian fluid in a channel with elastic walls", *Math. Model. Eng. Probl.* **7**:2 (2020), 315–323.

[35] D. F. Young, "Effect of a time dependent stenosis of flow through a tube", *J. Eng. Ind. Trans. ASME.* **90**:2 (1968), 248–254.

Received 20 Oct 2021. Revised 2 Nov 2021. Accepted 25 Mar 2022.

MALLINATH DHANGE: math.mallinath@bldeacet.ac.in
Department of Mathematics, BLDEA's VP Dr. PG Halakatti College of Engineering and Technology, Vijayapur, India

GURUNATH SANKAD: math.gurunath@bldeacet.ac.in
Department of Mathematics, BLDEA's VP Dr. PG Halakatti College of Engineering and Technology, Vijayapur, India

UMESH BHUJAKKANAVAR: umesh.bhujakkanavar@ritindia.edu
Department of Science and Humanities, Rajarambapu Institute of Technology, Islampur, India


MATHEMATICS AND MECHANICS OF COMPLEX SYSTEMS

msp.org/memocs

MEMOCS is a journal of the International Research Center for the Mathematics and Mechanics of Complex Systems at the Università dell'Aquila, Italy.

See inside back cover or msp.org/memocs for submission instructions.

The subscription price for 2022 is US $195/year for the electronic version, and $255/year (+$25, if shipping outside the US) for print and electronic. Subscriptions, requests for back issues and changes of subscriber address should be sent to MSP.

Mathematics and Mechanics of Complex Systems (ISSN 2325-3444 electronic, 2326-7186 printed) at Mathematical Sciences Publishers, 798 Evans Hall #3840, c/o University of California, Berkeley, CA 94720-3840 is published continuously online.

MEMOCS peer review and production are managed by EditFlow® from MSP.

PUBLISHED BY

mathematical sciences publishers

nonprofit scientific publishing

http://msp.org/

Mathematics and Mechanics of Complex Systems
vol. 10 no. 2 2022

Homogenization of a 2D two-component domain with an oscillating thick interface 103
Patrizia Donato and Klas Pettersson

Modeling of blood flow with stenosis and dilatation 155
Mallinath Dhange, Gurunath Sankad and Umesh Bhujakkanavar

Corrector results for space-time homogenization of nonlinear diffusion 171
Tomoyuki Oka

Dynamic Bergan–Wang theory for thick plates 191
Harm Askes and Alexandra R. Wallace

MEMOCS is a journal of the International Research Center for the Mathematics and Mechanics of Complex Systems at the Università dell'Aquila, Italy.